Research Article

A Compact, Bistatic Antenna System with Very High Interport Isolation for 2.4 GHz In-Band Full Duplex Applications

Haq Nawaz [ID],[1] **Nosherwan Shoaib** [ID],[2] **Ahmad Umar Niazi** [ID],[1]
and Shabbir Majeed Chaudhry [ID][3]

[1]*Electronics Engineering, University of Engineering and Technology (UET) Taxila, Sub-Campus Chakwal, Chakwal 48800, Pakistan*
[2]*Research Institute for Microwave and Millimeter-Wave Studies (RIMMS), National University of Sciences and Technology (NUST), Islamabad, Pakistan*
[3]*Electrical Engineering, University of Engineering and Technology (UET), Taxila 47050, Pakistan*

Correspondence should be addressed to Nosherwan Shoaib; nosherwan.shoaib@seecs.edu.pk

This paper presents a compact, dual polarized bistatic (two closely spaced transmit and receive radiators) patch antenna with excellent interport isolation performance. The presented antenna system employs differential receive mode operation for the cancellation of self-interference (SI) to achieve very high interport isolation for 2.4 GHz in-band full duplex (IBFD) applications. The presented antenna is based on two closely spaced radiators and a simple 3 dB/180° coupler for differentially excited receive mode operation. The 3 dB/180° coupler performs as a passive self-interference cancellation (SIC) circuit for the presented antenna. The small form-factor structure is realized through via interconnections between the receiving patch and SIC circuit. The prototype of the presented antenna characterizes better than 105 dB peak interport isolation. Moreover, the recorded interport isolation is more than 90 dB and 95 dB within 60 MHz and 40 MHz bandwidths, respectively. The measured gain and cross-polarization levels reflect superior radiation performance for the validation model of the proposed antenna. The presented antenna offers DC interport isolation too, which is required for active antenna applications. The novelty of this work is a compact (small form-factor) antenna structure with very high peak interport isolation along with wider SIC bandwidth as compared to previously reported antennas for full duplex applications.

1. Introduction

For the realization of in-band full duplex (IBFD) wireless communications with its full potentials, the RF coupling at receive chain resulting from its own transmitter must be fully suppressed [1–3]. This coupling from transmit (T_x) to receive (R_x) chain is termed as self-interference (SI) and overpowers the intended R_x signals. The achieved self-interference cancellation (SIC) levels are termed as the figure of merit for IBFD transceiver design [2, 3]. These SIC levels are directly related to the transmitted power and T_x bandwidth [4].

These high SIC levels for intended IBFD operation can be achieved through multiple SIC techniques at various stages across the transceiver including SIC at receiver's front end, analog/RF domain SIC, and the digital baseband SIC topologies [1–3]. Moreover, comparatively large amount of SIC levels should be achieved at receiver's front end (antenna stage) in order to preserve the dynamic range of analog to digital converter in R_x chain [1–3, 5]. In addition, achieving high SIC levels at receiver's front end will reduce the complexity of SIC topologies employed on subsequent stages across the R_x chain [1–3]. For example, as illustrated in Figure 1, for the case of transceiver with required isolation levels of 110 dB, if the antenna stage SIC is around 80 dB, only 30 dB SIC is required from SIC topologies employed at digital baseband stage to achieve the required aggregate SIC levels of 110 dB for the realization of
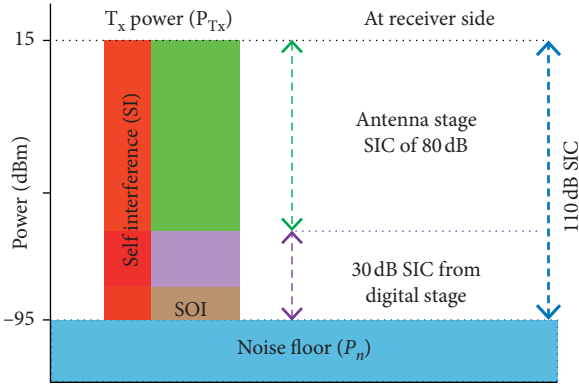
FIGURE 1: Achieving around 110 dB self-interference cancellation (SIC) for an IBFD transceiver with 80 dB and 30 dB SIC at antenna and digital baseband stages, respectively.

IBFD communication without using complex analog domain SIC techniques.

The bistatic antenna topology (separate elements for T_x and R_x modes) can be used for IBFD transceiver where the spatial domain isolation through interantenna spacing provides reduced coupling between T_x and R_x ports. However, the T_x and R_x elements should be tightly packed for compact antenna structure which limits the amount of spatial isolation. Moreover, the T_x and R_x operation can be realized through orthogonal polarization to exploit the intrinsic isolation of polarization diversity. However, the polarization isolation alone is not enough at antenna stage to meet the required aggregate SIC levels for IBFD operation [5–7]. In that case, analog or RF domain active SIC topologies can be used with dual polarized antennas to achieve additional interport isolation [8–11]. The performance of such SIC techniques is highly dependent on the characteristics of active SIC circuitry. Moreover, these SIC techniques are normally narrow band to provide SIC for few MHz bandwidths [8, 9].

The differential feeding or excitation is a very effective SIC mechanism (passive SIC) to obtain high port to port isolation without degradation in radiation characteristics of antennas. The differential excitation can be used either at one port (T_x/R_x) or at both T_x and R_x ports. Moreover, the differential excitation based near-field SIC techniques can achieve improved levels of interport isolation for IBFD monostatic (shared antenna) or bistatic (separate antenna) antenna systems [12–19]. In addition, the combination of differential excitation and balanced feeding networks is utilized to achieve improved isolation and reduced cross-polarization levels for dual polarized antennas. However, such antenna designs are mostly based on multilayered PCB structures and complex balanced feed networks [16–19]. The differential excitation based near-field SIC techniques utilize the two coupled signals from T_x port to perform the difference operation at R_x port. The achievable isolation levels through differential feeding are highly dependent upon the symmetry of T_x and R_x ports of IBFD antennas and the performance of employed differential feeding network (DFN). In addition, the propagation domain coupling between the radiating element(s) and DFN limits the

achievable SIC levels too [19]. The 3 dB/180° ring hybrid coupler (rat-race coupler) is considered a good choice as DFN due to its superior amplitude and out-of-phase balance response to achieve very high SIC levels [12, 13, 19].

The dual polarized antennas with high interport RF isolation along with DC isolation are required for active integrated antenna applications [20, 21]. Such antennas are also used for realization of retrodirective antenna arrays [22] or amplifying-reflect type of arrays [23]. Such antennas with DC interport isolation will avoid the DC blocking series capacitors required either in T_x or in R_x path. Consequently, the insertion loss resulting from such series capacitors will be avoided. The cross-polarized antennas with high interport decoupling can also mitigate the fading effects [24].

However, most of the previously reported bistatic IBFD antenna configurations have large dimensions or degraded levels of interport isolation levels when the spacing between the T_x and R_x elements is reduced [14]. Achieving the high isolation levels through the compact antenna structures without compromising its radiation performance and electrical dimensions is still a challenging task. The motivation of this work is to realize an IBFD antenna with high interport isolation through a small form-factor (reduced dimensions) antenna structure.

In this work, a 2.4 GHz bistatic antenna system based on two closely spaced (interelement spacing of $\lambda_o/4$), dual polarized patches are demonstrated with improved T_x-R_x isolation through differential R_x mode operation. The differentially driven SIC mechanism for presented antenna system is illustrated through design equations. A simple 3 dB/180° ring hybrid coupler with superior amplitude and out-of-phase balance characteristics has been used as DFN for effective SIC operation to achieve improved levels of interport isolation. The achieved isolation levels are provided through the combination of spatial isolation (path loss-based isolation), polarization diversity isolation, and isolation achieved through differential R_x mode operation for the presented dual polarized bistatic antenna system.

2. Differentially Driven 2.4 GHz Dual Polarized Bistatic Antenna

The proposed dual polarized 2.4 GHz bistatic antenna system is shown in Figure 2. It comprised two patches where one patch with a single port is intended for T_x mode and the second patch with two ports will be used for differentially driven R_x mode. Each port is matched with square radiating element through quarter wave ($\lambda_g/4$) transmission lines as depicted in Figure 2. Due to the symmetric dimensions of both patches, they resonate at the same frequency of 2.4 GHz for T_x and R_x modes. Both elements are closely spaced and interelement spacing is only $\lambda_o/4$, where λ_o (125 mm) is the free space wavelength at 2.4 GHz frequency. A 1.6 mm thick single-layered FR-4 substrate ($\varepsilon_r = 4.4$, tan $\delta = 0.02$) has been opted for the design of presented antenna system. Due to the symmetric placement of R_x patch with respect to T_x patch, the same amount of T_x power (self-interference) is coupled to each R_x port of the second radiating element.
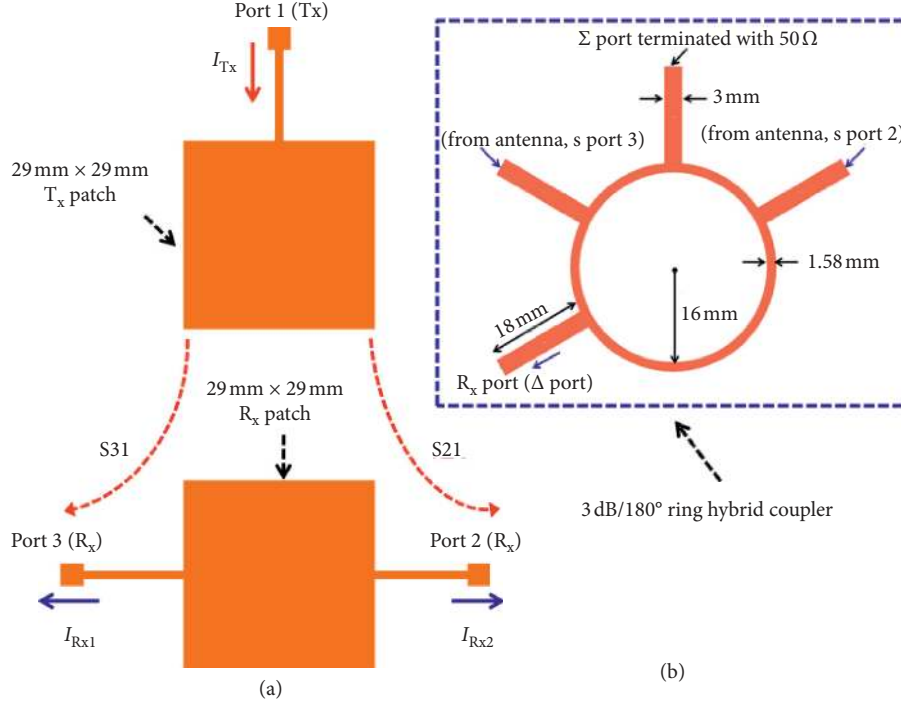
FIGURE 2: (a) The topology of dual polarized bistatic patch antenna system based on a single port transmit patch and two ports receive patch for differential receive mode operation to suppress the self-interference. (b) 3 dB/180° ring hybrid coupler as a SIC circuit.

Furthermore, both port 2 and port 3 (R_x ports) are cross polarized with respect to port 1 (T_x port). The polarization diversity and spatial separation provide around 47 dB isolation between each T_x-R_x pair of ports as endorsed through simulation results for the proposed antenna structure. The polarization isolation is around 37 dB at 2.4 GHz as reported in [5] and spatial isolation is 10 dB for physical separation (interelement distance) of 31.25 mm. Moreover, the interport isolation is better than 35 dB for 70 MHz bandwidth (10 dB return-loss bandwidth for each port). The proposed differentially driven operation through both R_x ports of the second patch can offer an effective suppression of SI (T_x leakage) at R_x port to obtain the additional isolation superimposed on inherent polarization, diversity isolation, and spatial isolation between T_x and R_x patches. This SIC mechanism can be illustrated through following signal flow analysis for the proposed, dual polarized IBFD bistatic antenna system.

As indicated in Figure 2, assume that S_{21} and S_{31} represent the magnitudes of interport coupling or T_x leakage to each R_x port, respectively. In that case, the currents flowing out of R_x ports (I_{Rx1} and I_{Rx2}) are related to T_x port current (I_{Tx}) through the following equations:

$$I_{Rx1} = I_{Tx} * S_{31},$$
$$I_{Rx2} = I_{Tx} * S_{21}. \tag{1}$$

If an ideal differential circuit (lossless power combiner with perfect amplitude balance and 180° phase balance characteristics) is connected at both R_x ports, the total current I_{Rx} (total leakage signal) at the output of differential circuit is given as follows:

$$I_{Rx} = \frac{1}{\sqrt{2}}\left(I_{Rx1} + e^{j180°} * I_{Rx2}\right) = \frac{I_{Tx}}{\sqrt{2}}\left(S_{31} - S_{21}\right). \tag{2}$$

From (2), the ratio of the T_x and R_x currents can be defined as

$$\frac{I_{Tx}}{I_{Rx}} = \frac{\sqrt{2}}{\left(S_{31} - S_{21}\right)}. \tag{3}$$

As evident from (3), the achievable port to port isolation levels for the proposed bistatic antenna system depend on the amplitude and out-of-phase balance properties of the differential network in addition to the RF coupling between T_x and both R_x ports (S_{21} and S_{31}). It is important to mention here that this coupling depends upon the polarization and free pace path loss between the two closely spaced patches.

As stated earlier, due to the symmetry of antenna structure, the same amount of T_x leakage should be generated at both R_x ports which will result in perfect SIC operation if an ideal DFN is employed to provide infinite T_x-R_x isolation. However, the coupled signals from T_x to R_x patch are dependent upon the environmental factors and manufacturing accuracy for the implemented antennas. Moreover, the propagation domain coupling between radiating elements and DFN degrades the SIC level too. Consequently, in practical scenarios, $S_{21} \approx S_{31}$ to offer very high SIC levels if a DFN with superior amplitude and out-of-phase balance characteristics is used for differential R_x mode operation. Moreover, tunable attenuator and phase shifter can be placed at the inputs of DFN to adjust the magnitudes and phases of S_{21} and S_{31} to satisfy the SIC conditions stated

in (3). This mechanism can be used to obtain the optimized T_x-R_x isolation through automatic tuning for practical scenarios.

The effects of the amplitude and out-of-phase errors (imbalances) of DFN on SIC capabilities can be analyzed through the subtraction of two sinusoidal signals as shown in Figure 3. Figure 3 plots the difference (in dB) between two signals for different values of amplitude and out-of-phase errors. The magnitude and phase errors correspond to the magnitude and phase response of employed DFN, while the resulting difference is termed as SIC levels. As obvious from Figure 3, the SIC potential of DFN relies totally on both magnitude and phase response of the DFN. In other words, the SIC levels are throttled to very low levels when the amplitude and an out-of-phase errors are increased. Consequently, a DFN with well-balanced amplitude and an out-of-phase response is essential to achieve improved SIC levels.

The simulated return losses and interport coupling results for the proposed bistatic antenna are presented in Figure 4. As can be seen from Figure 4, the ideal DFN with perfect amplitude and an out-of-phase characteristic can offer T_x-R_x isolation (negative of coupling) on excess of 100 dB within 75 MHz bandwidth (10 dB return-loss bandwidth of T_x/R_x patches). However, the isolation levels of better than 90 dB for 75 MHz bandwidth can be obtained when the proposed 3 dB/180° ring hybrid coupler is used as DFN. The coupler works as a differential power combiner to perform the intended (S_{31}–S_{21}) process at its difference port (Δ port) when it is excited through a pair of R_x ports of the antenna. As endorsed through simulation results, the proposed 3 dB/180° ring hybrid coupler has a well-balanced amplitude and out-of-phase balance response for intended bandwidth to offer better than 50 dB SIC levels. The proposed 3 dB/180° ring hybrid coupler and its dimensions are shown in Figure 2, but its simulation results are not presented here for brevity.

The simulated T_x and differentially excited R_x mode radiation characteristics of the proposed dual polarized bistatic antenna system are presented in Figure 5. The simulated results in Figure 5 demonstrate the vertical polarization for T_x port excitation and horizontal polarization for differentially excited R_x mode. As evident from Figure 5, the radiation performance of the antenna is not affected by differential excitation, as the E-field (E_x) components generated by differential feeding are additive as detailed in [15] and given by (4) for horizontal polarization. The differential feeding also suppresses the higher order modes to offer improved polarization purity or reduced cross-polarization levels for patch antenna [25].

$$\mathbf{E}_{Rx} = \mathbf{E}_{\mathbf{R}x1} + e^{j180°}\mathbf{E}_{\mathbf{R}x2} = \mathbf{E}_{\mathbf{r}}(\widehat{X}) - \mathbf{E}_{\mathbf{r}}(-\widehat{X}) = 2\mathbf{E}_{\mathbf{r}}(\widehat{X}), \quad (4)$$

where $\widehat{X}$ is unit vector along the x-axis and $\mathbf{E}_{\mathbf{r}}$ represents the amplitude of electric field.
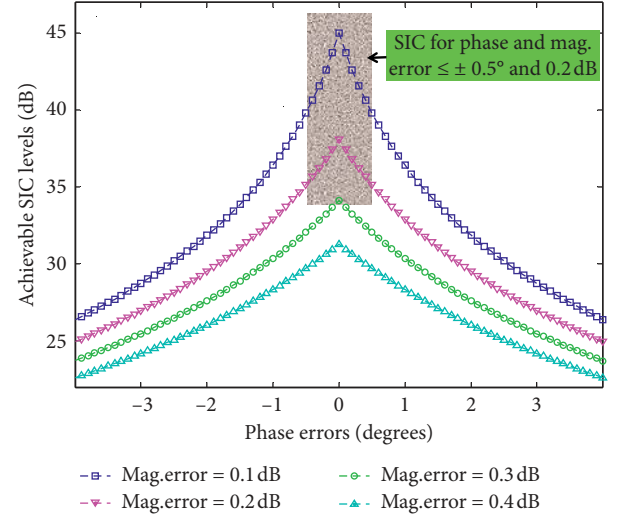

FIGURE 3: The effects of the amplitude and out-of-phase errors or imbalances of DFN on the achievable SIC levels.
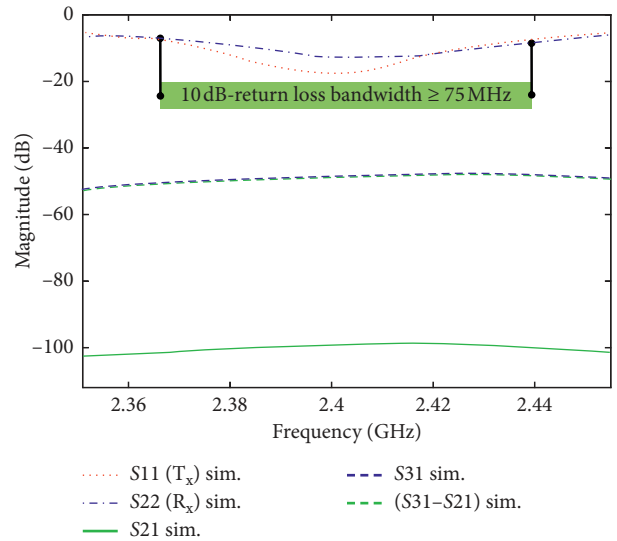

FIGURE 4: The simulated S-parameters for proposed bistatic antenna system having single port T_x patch and dual port R_x patch.

3. Antenna Implementation for Experimental Demonstration

For experimental demonstration, the 2.4 GHz ring hybrid coupler and radiating structure (antenna elements) were etched on 1.6 mm thick FR-4 substrate ($\varepsilon_r = 4.4$, tan δ = 0.02). The DFN (ring hybrid) was connected at R_x ports through holes with ground plane sandwiched between two substrate layers. Both structures are electromagnetically isolated due to interlayer ground plane. Two SMA connectors were soldered at the respective T_x and R_x (port of coupler) ports. The sum (Σ) port of the differential circuit (ring hybrid coupler) is terminated in a 50 Ω SMD resistor in order to avoid reflections. The overall size of the implemented prototype is 115 mm × 68 mm × 3.2 mm as shown in
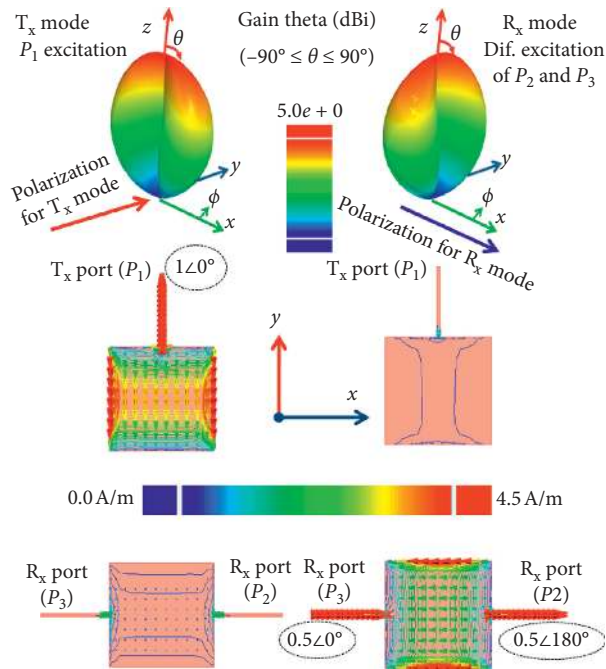
FIGURE 5: The simulated surface currents intensity and 3D gain patterns at $f = 2.4$ GHz for T_x mode and differential driven R_x mode through respective port excitation.

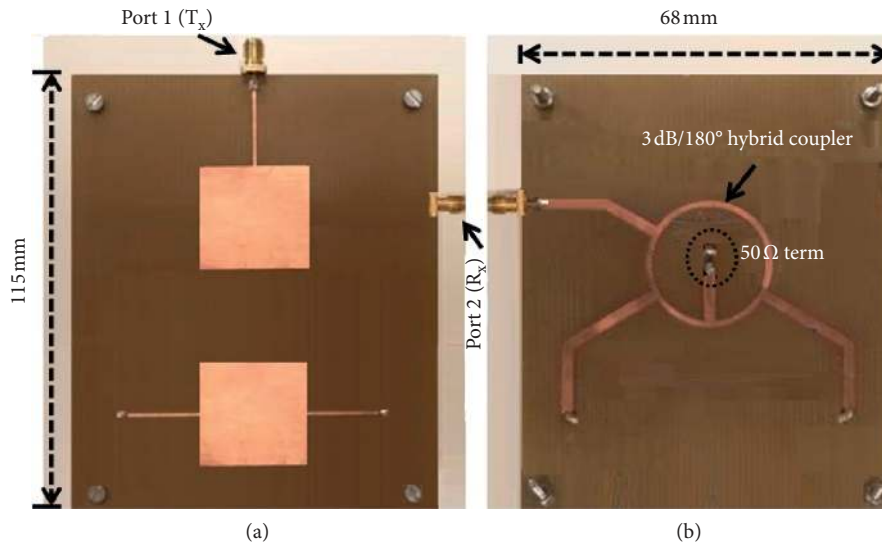(a)   (b)

FIGURE 6: The validation model (prototype) of 2.4 GHz differential fed IBFD bistatic patch antenna implemented on double layered FR-4 substrate. (a) Top side. (b) Bottom side.

Figure 6. It is important to mention here that the DFN and radiating elements can be etched on the same side of a single-layered printed circuit board (PCB). However, this will result in a bistatic antenna system with larger dimensions or sizes. Moreover, the direct electromagnetic coupling between the two structures will degrade the interport isolation performance of the IBFD antenna. The implemented prototype can be interfaced with respective T_x and R_x chains of the full duplex transceiver. Moreover, the T_x and R_x ports of the presented antenna can be interchanged without affecting the interport isolation characteristics. However, the T_x and R_x ports of antenna connected to remote radio (transceiver) should be interchanged too in order to match the polarization for the respective links at local and remote nodes or transceivers [15, 19].

The implemented bistatic antenna was characterized through return loss and interport isolation measurements in the antenna chamber. The simulated and measured S_{11} (T_x port), S_{22} (R_x port), and S_{21} (T_x to R_x port coupling or negative isolation) results for physical model are presented in Figure 7.
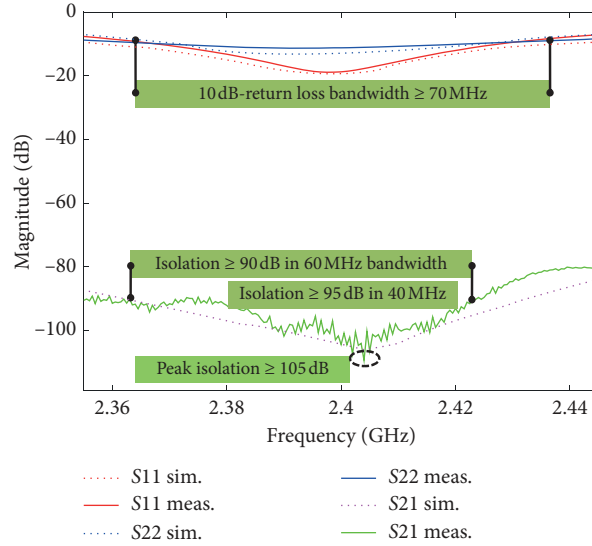
FIGURE 7: The simulated and experimentally recorded S_{11}, S_{22}, and interport coupling results (S_{21}) for implemented dual polarized bistatic antenna.

As clear from measurement results, the input (T_x port) and output (R_x port) return losses for implemented antenna are better than 18 dB and 12 dB at the center resonating frequency of 2.42 GHz. In addition, the validation model or prototype achieves the overlapping 10 dB return-loss bandwidth of 70 MHz (2.365 GHz to 2.435 GHz) for both input and output ports. The measured isolation (negative of coupling) for implemented antenna was determined as better than 90 dB for 60 MHz bandwidth which spans over 2.365 GHz to 2.425 GHz. Furthermore, higher than 95 dB isolation has been recorded for 40 MHz bandwidth which ranges from 2.38 GHz to 2.42 GHz as clearly marked in Figure 7. The measured peak isolation is in excess of 105 dB at 2.405 GHz frequency as indicated in Figure 7. Consequently, for the 60 MHz bandwidth, 45–50 dB isolation is contributed by SIC circuit on the top of polarization diversity and spatial isolation.

The radiation performance of the implemented prototype was endorsed through the gain measurements for each polarization or port excitation. The simulated and measured two-dimensional (2-D) copolarized and cross-polarized E-plane gain patterns for validation model are presented in Figure 8. These radiation patterns have been recorded at 2.405 GHz frequency for excitation of the respective T_x (port 1) and R_x (differential port, i.e., port 2) ports. For the gain measurements of T_x mode, the R_x port of antenna was terminated in a 50 Ω load and T_x port was excited through a signal generator. Similarly, for gain measurements of R_x mode, the   port of coupler was excited and T_x port was connected with a 50 Ω termination. The sum (Σ) of coupler is already terminated in 50 Ω SMD resistor. As clearly indicated and evident from Figure 8, the recorded gains for intended polarizations are better than 4.8 dBi for each of T_x and R_x ports. As expressed through experimental results, the low insertion loss of DFN employed for differentially driven mode does not degrade the radiation performance of R_x. Moreover, the gain improvements due to differential
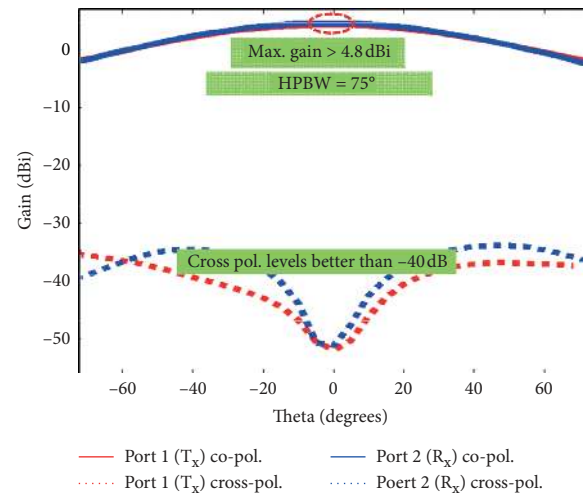

FIGURE 8: The measured T_x and R_x modes copolarization and cross-polarization gain levels for the presented antenna at 2.405 GHz frequency.

excitation compensate the resulting insertion loss of DFN. Consequently, almost similar measured gain levels have been observed for both T_x and R_x polarizations. Moreover, the recorded/measured cross-polarization levels for the implemented antenna are suppressed to better than −40 dB for half power beam width (HPBW) of 75 degrees. These results reflect the improved gain levels for intended polarization along with excellent polarization purity for each of T_x and R_x modes.

The interport isolation performance and dimensions of presented antenna are compared with some of the previously reported 2.4 GHz dual polarized IBFD antennas [14, 26–30] as detailed in Table 1.

It is obvious from this comparison table, that the presented dual polarized IBFD antenna system offers better T_x-R_x interport isolation versus SIC bandwidth performance as

TABLE 1: The comparison of interport isolation and dimensions of presented antenna with some of the previously reported dual polarized, full duplex antennas [14, 26–30].

Reference	Center freq. (GHz)	Peak isolation (dB)	Isolation (dB)/B.W. (MHz)	Antenna size $(L^*W) * \lambda_o$	SIC topology
[14]a	2.5	70	64/110	(1.1*0.6)	DFN
[14]b	2.5	75	60/160	(1.0*0.6)	DFN
[26]	2.5	≥75	40/220	(1.1*0.7)	Polarization diversity
[27]	2.45	≥50	30/300	(1.2*0.8)	Analog SIC
[28]	2.45	≥90	40/65	Not applicable	Analog SIC
[29]	2.4	~50	47/75	(1.5×1.4)	DFN
[30]	3.35	≥55	40/250	Not given	Using circulators
This work	2.40	≥105	90/60 and 95/40	(0.9*0.6)	Polarization diversity + DFN

compared to the previously reported antenna designs in addition to reduced dimensions $(0.9\lambda_o \times 0.6\lambda_o)$/small form factor of our antenna structure. Moreover, the presented antenna system provides very high peak isolation compared to the closely spaced antennas which were reported earlier. The 60 MHz SIC (isolation) bandwidth with more than 90 dB isolation makes this antenna a promising choice for deployment in 2.4 GHz ISM band applications having three full duplex bidirectional channels. The potential applications include 2.4 GHz wireless local area network (WLAN) with 20 MHz bandwidth for each of the three full duplex channels, where the propagation domain isolation between forward and reverse channel is achieved through polarization diversity.

4. Conclusion

A compact $(0.9\lambda_o \times 0.6\lambda_o)$, dual port, bistatic antenna system with high port to port isolation is demonstrated for 2.4 GHz same frequency full duplex or IBFD wireless applications. The presented antenna is comprised of two closely spaced dual polarized patches. It employs a nicely balanced 3 dB/180° ring hybrid coupler as a differential feeding network for R_x mode to achieve high port-to-port isolation through an effective SIC operation. The differential feeding based SIC operation is also described through mathematical equations in order to illustrate the effects of amplitude and phase imbalances of differential feeding network on the achievable SIC levels. The differential feeding network offers around 45–50 dB SIC on the top of 45–50 dB isolation provided by polarization diversity (dual polarization) and interelement spacing. The presented antenna system offers better isolation characteristics compared to the previously reported full duplex antennas. The implemented antenna offers compact size along with SIC capabilities better than 90 dB for 60 MHz bandwidth and can be readily integrated with 2.4 GHz radios for realization of low power full duplex wireless operation, without using additional complex SIC topologies. In addition to high interport RF isolation, the presented antenna also offers DC interport isolation (as no conduction path exists between T_x and R_x ports). The DC interport isolation is required for various active antenna applications. Thus, the presented antenna can be employed for such active antenna applications without using series capacitors in T_x path. Consequently, the RF power loss resulting from such series capacitors will be removed.

Data Availability

The data used to support the design and validation of the presented antenna are available from the corresponding author on request.

Conflicts of Interest

The authors declare that they have no conflicts of interest.

References

[1] D. Bharadia, E. McMilin, and S. Katti, "Full duplex radios," in *Proceedings of the ACM SIGCOMM 2013*, Hong Kong, China, August 2013.

[2] J. Marašević, J. Zhou, H. Krishnaswamy, Y. Zhong, and G. Zussman, "Resource allocation and rate gains in practical full-duplex systems," *IEEE/ACM Transactions on Networking*, vol. 25, no. 1, pp. 292–305, 2017.

[3] D. Korpi, T. Riihonen, V. Syrjala, L. Anttila, M. Valkama, and R. Wichman, "Full-duplex transceiver system calculations: analysis of ADC and linearity challenges," *IEEE Transactions on Wireless Communications*, vol. 13, no. 7, pp. 3821–3836, 2014.

[4] L. Anttila, D. Korpi, V. Syrjälä et al., "Cancellation of power amplifier induced nonlinear self-interference in full-duplex transceivers," in *Proceedings of the 2013 Asilomar Conference on Signals, Systems and Computers*, pp. 1193–1198, Pacific Grove, CA, USA, November 2013.

[5] H. Nawaz and I. Tekin, "Three dual polarized 2.4 GHz microstrip patch antennas for active antenna and in-band full duplex applications," in *Proceedings of the 2016 16th Mediterranean Microwave Symposium (MMS)*, pp. 1–4, Abu Dhabi, UAE, November 2016.

[6] M. S. Amjad, H. Nawaz, K. Özsoy, O. Gurbuz, and I. Tekin, "A low-complexity full-duplex radio implementation with a single antenna," *IEEE Transactions on Vehicular Technology*, vol. 67, no. 3, pp. 2206–2218, 2018.

[7] C. Younkyu, J. Seong-Sik, D. Ahn et al., "High isolation dual-polarized patch antenna using integrated defected ground structure," *IEEE Microwave and Wireless Components Letters*, vol. 14, no. 1, pp. 4–6, 2004.

[8] H. Nawaz and I. Tekin, "Dual port single patch antenna with high interport isolation for 2.4 GHz in-band full duplex wireless applications," *Microwave and Optical Technology Letters*, vol. 58, no. 1, pp. 1756–1759, 2016.

[9] H. Nawaz, Ö. Gürbüz, and I. Tekin, "High isolation slot coupled antenna with integrated tunable self-interference

cancellation circuitry," *Electronics Letters*, vol. 54, no. 23, pp. 1311-1312, 2018.

[10] K. E. Kolodziej, J. G. McMichael, and B. T. Perry, "Multitap RF canceller for in-band full-duplex wireless communications," *IEEE Transactions on Wireless Communications*, vol. 15, no. 6, pp. 4321–4334, 2016.

[11] H. Nawaz, Ö. Gürbüz, and I. Tekin, "2.4 GHz dual polarised monostatic antenna with simple two-tap RF self-interference cancellation (RF-SIC) circuitry," *Electronics Letters*, vol. 55, no. 6, pp. 299-300, 2019.

[12] M. Yilan, H. Ayar, H. Nawaz, O. Gurbuz, and I. Tekin, "Monostatic antenna in-band full duplex radio: performance limits and characterization," *IEEE Transactions on Vehicular Technology*, vol. 68, no. 5, pp. 4786–4799, 2019.

[13] H. Nawaz and I. Tekin, "Dual-polarized, differential fed microstrip patch antennas with very high interport isolation for full-duplex communication," *IEEE Transactions on Antennas and Propagation*, vol. 65, no. 12, pp. 7355–7360, 2017.

[14] G. Chaudhary, J. Jeong, and Y. Jeong, "Differential fed antenna with high self-interference cancellation for in-band full-duplex communication system," *IEEE Access*, vol. 7, pp. 45340–45348, 2019.

[15] H. Nawaz and I. Tekin, "Double-differential-fed, dual-polarized patch antenna with 90 dB interport RF isolation for a 2.4 GHz in-band full-duplex transceiver," *IEEE Antennas and Wireless Propagation Letters*, vol. 17, no. 2, pp. 287–290, 2018.

[16] K. Luo, W.-P. Ding, Y.-J. Hu, and W.-Q. Cao, "Design of dual-feed dual-polarized microstrip antenna with high isolation and low cross polarization," *Progress in Electromagnetics Research Letters*, vol. 36, pp. 31–40, 2013.

[17] H. Nawaz and A. Umar Niazi, "A compact proximity-fed 2.4 GHz monostatic antenna with wide-band SIC characteristics for in-band full duplex applications," *International Journal of RF and Microwave Computer-Aided Engineering*, vol. 30, no. 3, Article ID e22087, 2019.

[18] C. Deng, Y. Li, Z. Zhang, and Z. Feng, "A wideband high-isolated dual-polarized patch antenna using two different balun feedings," *IEEE Antennas and Wireless Propagation Letters*, vol. 13, pp. 1617–1619, 2014.

[19] H. Nawaz, M. A. Basit, and F. Shaukat, "Dual polarized, slot coupled monostatic antenna with high isolation for 2.4 GHz full duplex applications," *Microwave and Optical Technology Letters*, vol. 62, no. 3, pp. 1291–1298, 2019.

[20] K. Chang, R. A. York, P. S. Hall, and T. Itoh, "Active integrated antennas," *IEEE Transactions on Microwave Theory and Techniques*, vol. 50, no. 3, pp. 937–944, 2002.

[21] H. Nawaz and M. A. Basit, "Single layer, dual polarized, 2.4 GHz patch antenna with very high Rf isolation between dc isolated Tx-Rx ports for full duplex radio," *Progress in Electromagnetics Research Letters*, vol. 85, pp. 65–72, 2019.

[22] C. Luxey and J.-M. Laheurte, "A retrodirective transponder with polarization duplexing for dedicated short range communications," *IEEE Transactions on Microwave Theory and Techniques*, vol. 47, pp. 1910–1915, 1999.

[23] M. E. Bialkowski and H. J. Song, "Investigations into a power-combining structure using a reflectarray of dual-feed aperture-coupled microstrip patch antennas," *IEEE Transactions on Antennas and Propagation*, vol. 50, no. 6, pp. 841–849, 2002.

[24] C. Puente, J. Anguera, and C. Borja, "Dual-band dual-polarized antenna array," US Patent 6,937,206, World Intellectual Property Organization, Geneva, Switzerland, 2001.

[25] X.-L. Liang, S.-S. Zhong, and W. Wang, "Design of a dual-polarized microstrip patch antenna with excellent polarization purity," *Microwave and Optical Technology Letters*, vol. 44, no. 4, pp. 329–331, 2005.

[26] X. Wang, W. Che, W. Yang, W. Feng, and L. Gu, "Self-interference cancellation antenna using auxiliary port reflection for full-duplex application," *IEEE Antennas and Wireless Propagation Letters*, vol. 16, pp. 2873–2876, 2017.

[27] H. Makimura, K. Nishimoto, T. Yanagi, T. Fukasawa, and H. Miyashita, "Novel decoupling concept for strongly coupled frequency-dependent antenna arrays," *IEEE Transactions on Antennas and Propagation*, vol. 65, no. 10, pp. 5147–5154, 2017.

[28] S. Khaledian, F. Farzami, B. Smida, and D. Erricolo, "Inherent self-interference cancellation for in-band full-duplex single-antenna systems," *IEEE Transactions on Microwave Theory and Techniques*, vol. 66, no. 6, pp. 2842–2850, 2018.

[29] H. Nawaz, A. U. Niazi, M. Abdul Basit, and M. Usman, "Single layer, differentially driven, LHCP antenna with improved isolation for full duplex wireless applications," *IEEE Access*, vol. 7, pp. 169796–169806, 2019.

[30] M. Biedka, Y. E. Wang, Q. M. Xu, and Y. Li, "Full-duplex RF front ends: from antennas and circulators to leakage cancellation," *IEEE Microwave Magazine*, vol. 20, no. 2, pp. 44–55, 2019.